

Tunable spin polarization in a two-dimensional electron gas modulated by a ferromagnetic metal stripe and a Schottky metal stripe

Feng Zhai* and H. Q. Xu†

Division of Solid State Physics, Lund University, P. O. Box 118, S-221 00 Lund, Sweden

Yong Guo

Department of Physics, Tsinghua University, Beijing 100084, China

(Received 4 March 2004; revised manuscript received 17 May 2004; published 13 August 2004)

We report on a theoretical study of the spin-dependent electron transport in a two-dimensional electron gas (2DEG) modulated by a stripe of ferromagnetic metal and a stripe of Schottky metal in a parallel configuration. It is shown that a device consisting of a 2DEG and a single ferromagnetic metal stripe with magnetization parallel to the current direction possesses an intrinsic symmetry and does not give spin-polarized current. The symmetry is broken in the device with the double metal stripe structure. The spin-dependent transmission and conductance of the device are calculated. It is shown that highly spin-polarized electron transport can be achieved in this structure. It is also shown that the spin polarity of the electron transport can be switched by a voltage applied to the Schottky metal stripe. The underlying physical mechanism of the results is discussed in terms of spin-dependent tunneling process in the device.

DOI: 10.1103/PhysRevB.70.085308

PACS number(s): 73.40.Gk, 73.23.Ad, 72.25.Dc, 75.75.+a

The incorporation of magnetic elements into semiconductors has attracted great current interest because of both rich physics in the system and its promising applications.^{1–21} For ferromagnetic metal (FM)-semiconductor (SC) heterostructures, one of the special focuses is on the problem of a rather low spin-injection efficiency² arising from the conductance mismatch between FM and SC materials.³ Recent experiments have demonstrated solutions of this problem by introducing diluted magnetic semiconductors as a spin aligner^{4,5} and by adding a tunneling barrier.^{6,7} Meanwhile, many efforts have been made towards the realization of an efficient source of spin-polarized electrons.

Another kind of combination of FM and SC materials, usually called magnetic barrier (MB) nanostructures,⁸ is realized by depositing a FM material on top of a near-surface two-dimensional electron gas (2DEG) formed in a modulation-doped semiconductor heterostructure. The FM material provides a magnetic field which can influence locally the motion of the electrons in the semiconductor heterostructure. The effects caused by the MBs have been studied extensively in the last decade,⁹ and the feasibility of spin filtering in MB nanostructures has been discussed.^{10–16} A simple, experimentally attractive proposal for spin devices was to exploit a single FM stripe on top of a 2DEG.^{10,11} By the application of a magnetic field, the magnetization of the FM stripe can be made parallel to the 2DEG plane and, at the same time, perpendicular to the FM stripe, creating a magnetic field with an antisymmetric profile in the 2DEG. Recent calculations have shown, however, that under this antisymmetric magnetic field condition, no spin filtering can occur.^{11–14} In the present work an intrinsic symmetry in the single FM stripe structure is revealed. It will be shown that the symmetry can be broken and thus spin filtering can be achieved by placing a Schottky normal-metal (NM) stripe parallel to the FM stripe on top of the 2DEG. It will also be shown that not only the amplitude of the polarization but

also its sign varies with the electrical barrier (EB) height created by the NM stripe. Therefore, the considered device can be employed as a source of spin-polarized electrons, whose polarity can be switched by a voltage applied to the NM stripe.

The system under consideration is a 2DEG in the (x, y) plane subject to modulations by a FM stripe and a Schottky NM stripe as sketched in Fig. 1(a). Assume that the magnetic field provided by the FM stripe, $B_z(x)$, and the electrical potential induced by the Schottky stripe, $U(x)$, are homogeneous in the y direction and vary only along the x axis. The motion of an electron in such a modulated 2DEG system can be described by the single-particle Hamiltonian,

$$H = \frac{1}{2m^*}[\mathbf{P} + e\mathbf{A}(\mathbf{x})]^2 + U(x) + \frac{1}{2}g^* \mu_B \sigma_z B_z(x), \quad (1)$$

where m^* , \mathbf{P} and g^* are the effective mass, momentum and effective g -factor of the electron, $\mu_B = e\hbar/2m_0$ is the Bohr magneton (m_0 is the free electron mass), and σ_z represents the z -component of the electron spin (± 1 or \uparrow, \downarrow). $\mathbf{A}(\mathbf{x}) = A_y(x)\mathbf{e}_y$ is the magnetic vector potential under the Landau gauge. For convenience we express all quantities in dimensionless units by means of two characteristic parameters, i.e., cyclotron frequency $\omega_c = eB_0/m^*$ and magnetic length $l_{B_0} = \sqrt{\hbar/eB_0}$ (B_0 being some typical magnetic field).

Because of the translational invariance of the system along the y direction, the total electronic wave-function can be written as $\Phi(x, y) = e^{ik_y y} \Psi(x)$, where k_y is the transverse wave vector. $\Psi(x)$ satisfies a reduced one-dimensional Schrödinger equation,

$$-\frac{1}{2} \frac{d^2 \Psi}{dx^2} + \left\{ \frac{[k_y + A_y(x)]^2}{2} + U(x) + (g^* m^* / 4m_0) B_z(x) \sigma_z \right\} \Psi = E \Psi, \quad (2)$$

from which the transmission probability $T = T(E, k_y, \sigma_z)$ for

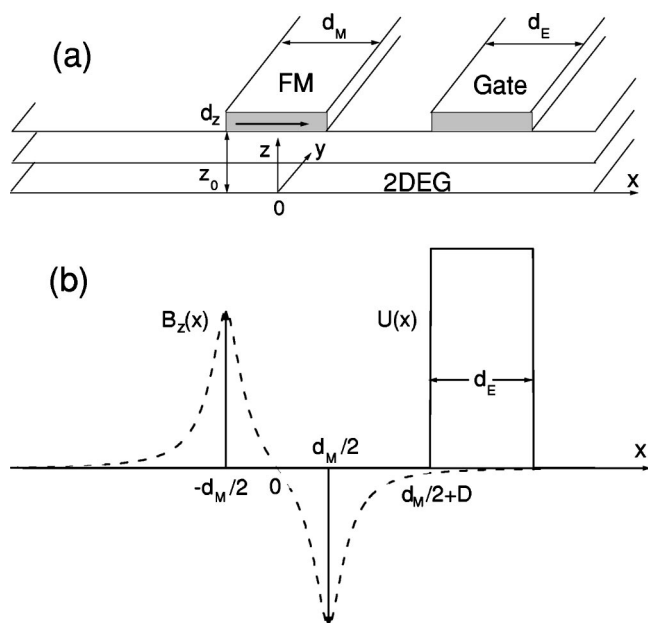


FIG. 1. (a) Schematic illustration of the spin device with a double metal stripe structure. On top of a 2DEG, a FM stripe and a Schottky NM stripe are placed in a parallel configuration. The magnetization of the FM stripe is assumed to be along the current direction (the x -direction). (b) Magnetic field and electric potential profiles exploited in this work. A simple square form is assumed for the electrical potential under the Schottky NM gate. For the magnetic field generated by the FM stripe, both a simplified (solid line) and a realistic (dashed line) profile are considered.

incident electrons with energy E , wave vector k_y , and spin orientation σ_z can be determined by means of the scattering matrix method.²² The conductance at zero temperature is calculated from⁸

$$G_{\sigma_z}(E_F) = G_0(E_F) \int_{-\pi/2}^{\pi/2} T(E_F, \sqrt{2E_F} \sin \theta, \sigma_z) \cos \theta d\theta, \quad (3)$$

where θ is the incident angle relative to the x direction. The up- and down-spin conductance components, G_{\uparrow} and G_{\downarrow} , as well as the total conductance, $G_{\text{tot}} = G_{\uparrow} + G_{\downarrow}$, are presented in units of $G_0(E_F) = e^2 m^* v_F L_y / h^2$, where L_y is the length of the structure in the y direction and v_F the Fermi velocity. The spin polarization can be characterized by the relative difference between the spin-up and spin-down conductances at the Fermi energy,

$$P_G = (G_{\uparrow} - G_{\downarrow}) / (G_{\uparrow} + G_{\downarrow}). \quad (4)$$

Many previous studies have focused on spin-dependent electron transport in a 2DEG modulated by a single FM stripe.^{10,11,15} The motion of a spin-half electron in such a system can be described by the Hamiltonian given in Eq. (1) without the electrical potential term describing the influence of the Schottky NM stripe. It is usually the case that the presence of the spin-field interaction [the last term in Eq. (1)] introduces spin polarization in the current.^{12,13,16} However, it is very important to notice that this is true only when there is not any symmetry leading to the degeneracy of spin-up and

spin-down states in the system. In a 2DEG system modulated by a single FM stripe with its magnetization along the current direction (the x -direction), the Hamiltonian is invariant under the operation of $\hat{T}\hat{R}_x\hat{R}_y$, where $\hat{T} = -i\hat{\sigma}_y K$, with K being the complex conjugation, is the time-reversal operator, and \hat{R}_x (\hat{R}_y) is the reflection operator, $x \rightarrow -x$ ($y \rightarrow -y$). This symmetry implies that the states with wave functions $\Phi(x, y) = e^{ik_y y} \Psi_{\sigma_z}(x)$ and $\Phi'(x, y) = \hat{T}\hat{R}_x\hat{R}_y \Phi(x, y)$ have the same eigenenergy. It can be easily verified that under the operation of $\hat{T}\hat{R}_x\hat{R}_y$, a spin-up state, $e^{ik_y y} \Psi_{\uparrow}(x)$, transforms to a spin-down state, $e^{ik_y y} \Psi_{\downarrow}(x)$, and a spin-down state, $e^{ik_y y} \Psi_{\downarrow}(x)$, transforms to a spin-up state, $e^{ik_y y} \Psi_{\uparrow}(x)$. Thus the spin-up and spin-down states with the same wave vector k_y are degenerate, and the transmission probability is spin-independent, $T(E, k_y, \sigma_z) = T(E, k_y, -\sigma_z)$. As a result, there is no spin polarization in the electron transport through the single FM stripe system in the linear response regime. To obtain a finite spin-polarization signal from the system, the symmetry under the operation of $\hat{T}\hat{R}_x\hat{R}_y$ should be broken, which, fortunately, can be easily done. One can, for example, break the symmetry by placing a Schottky NM stripe parallel to the FM stripe on top of the 2DEG, as shown in Fig. 1. Below, we present our numerical calculations for the 2DEG system with modulation by the double metal stripe.

Let us first consider a structure with simplified magnetic-field and electric potential profiles as depicted in Fig. 1(b) (solid line). It consists of a double-spike-like MB with strength B and distance d_M , and a rectangular EB with height U and width d_E , separated by a distance D . In our numerical calculation, the InAs system is taken as the 2DEG material ($g^* = 15$ and $m_{\text{InAs}}^* = 0.024m_0$) and the reduced units are $l_{B_0} = 81$ nm and $E_0 = \hbar\omega_c = 0.48$ meV, corresponding to $B_0 = 0.1$ T.

The device in discussion relies on the spin dependence of resonant tunneling due to the symmetry breaking. To obtain a quantitative feeling about this, in Fig. 2 we plot the transmission probability calculated as a function of the incident energy E for spin-up (T_{\uparrow}), spin-down (T_{\downarrow}) and spinless (T_0) electrons. The structure parameters were set at $B=6$ and $U=8$, and the transverse wave vector was set to be $k_y=0$ and ± 2 . It is seen that in comparison with the case of $k_y=-2$, the transmission for $k_y \geq 0$ is rather small in the considered energy region and is thus expressed in the logarithmic scale [Figs. 2(a) and 2(b)]. This result can be understood with the use of the figure shown in the inset of Fig. 2(a), where the one-dimensional effective potential (without including the Zeeman term) for electrons with the three different k_y values is shown [cf. Eq. (2)]. An electron with a positive k_y value will see a higher potential barrier due to the presence of a magnetic vector potential than that with a negative wave vector k_y , and thus has a smaller transmission probability through the structure. The transmission for electrons with $k_y=-2$ is shown in Fig. 2(c). It is seen that the transmission is significantly enhanced. This is as expected because effectively the electrons see a lower magnetic vector potential barrier in this case. It is also seen in Figs. 2(a)–2(c) that there exist sharp resonances in the calculated transmissions. The presence of the Zeeman coupling term changes the positions

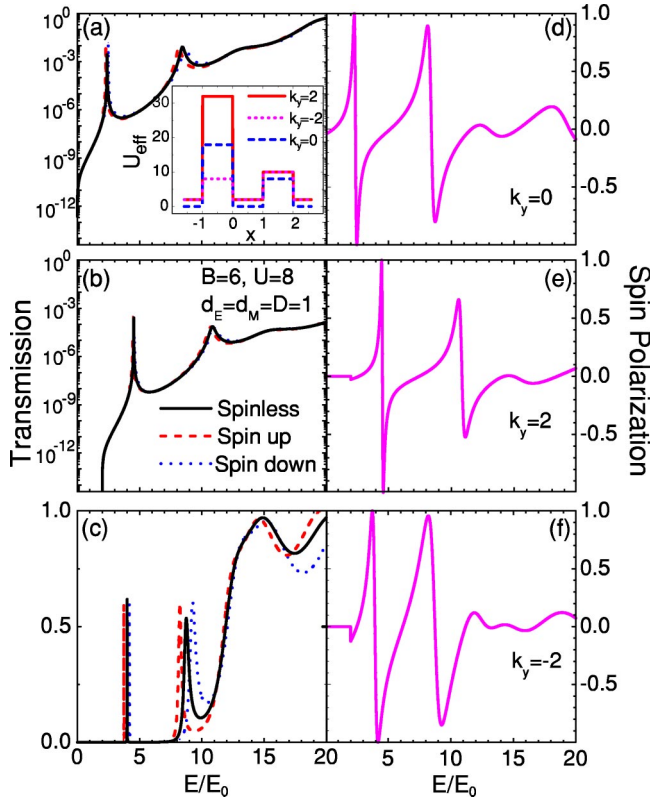


FIG. 2. Left panel: Transmission as a function of incident energy for spinless (solid line), spin-up (dashed line) and spin-down (dotted line) electrons with the transverse wave vector of (a) $k_y=0$, (b) $k_y=2$ and (c) $k_y=-2$, for the double metal stripe device with the simplified magnetic field profile as shown by the double spike line in Fig. 1(b). The inset in (a) shows the effective one-dimensional potentials seen by a spinless electron with different transverse wave vectors k_y . Device parameters used in the calculations are $d_M=d_E=D=1$, $B=6$ and $U=8$. Right panel: Corresponding spin polarization of the transmissions, P_T , for electrons with the three different transverse wave vectors k_y .

of the resonances, which shift towards the low-energy region for spin-up electrons and to the high-energy region for spin-down electrons. Therefore, one can expect a remarkable difference in the transmission for electrons with opposite spin orientations, at the resonant energies. The difference between the spin-up and spin-down electron transmissions can be revealed by the polarization of the transmitted beam, defined as $P_T=(T_\uparrow-T_\downarrow)/(T_\uparrow+T_\downarrow)$. From Figs. 2(d)–2(f) one can see that the polarization of electrons changes its sign when the incident energy varies from a spin-up resonant peak to its corresponding spin-down one. The amplitude of P_T can be very large at resonant energies. In the high energy region, T_\uparrow and T_\downarrow are large and their relative difference is small.

The spin-dependent transmission features demonstrated above should be reflected in the measurable quantity, the conductance G , which is obtained by integration of the transmission of electrons over the incident angle as in Eq. (3). Figure 3 shows the conductances for spin-up and spin-down electrons as well as their difference versus the Fermi energy for three different EB heights, $U=0$ and ± 8 . In

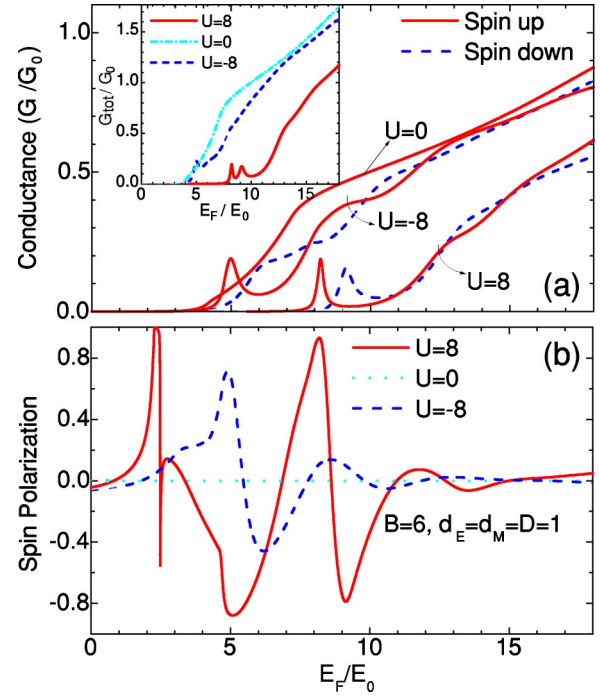


FIG. 3. Spin-dependent conductance and spin polarization, P_G , as a function of the Fermi energy for the same device as in Fig. 2. The total conductance is plotted in the inset. Three electrical potential strengths, $U=0$ and $U=\pm 8$, are considered. Other device parameters assumed are $d_M=d_E=D=1$ and $B=6$, the same as in Fig. 2.

the case of $U=0$, only the potential barrier due to the magnetic stripe is present, and the conductance of spin-up electrons, G_\uparrow , coincides completely with the conductance of spin-down electrons, G_\downarrow , as expected. The two conductances are generally lowered when U is finite. However, for a negative value of U (e.g., $U=-8$), the spin-up electron conductance, as well as the total conductance, may exceed the corresponding values seen in the case of $U=0$, due to the spin-dependent resonant enhancement [see Fig. 3(a) and the inset]. When E_F changes from a resonant peak to an adjacent valley, the conductance polarization is switched, as depicted by the dashed line in Fig. 3(b). As for the positive U , the polarization shows oscillations with larger amplitudes. Moreover, in the low energy region there exists a small plateau with nearly 100% polarization although the corresponding conductance in the energy region is rather small. The polarization plateau is associated with resonant tunneling through states formed in an effective double-barrier structure (cf. Fig. 2). It is also interesting to note that in the case of $U=8$, the spin-up electron conductance peak at energy around $E_F=8$ is well separated from its corresponding spin-down one. Thus the two peaks can be discerned in the total conductance, as shown in the inset of Fig. 3(a). Therefore the $G_{\text{tot}}-E_F$ measurement alone would provide an experimental evidence for spin polarization in the electron transport in the device.

A tunable spin-polarized source is desirable for spintronic applications.¹⁷ It is thus necessary to explore in more details the tunability of spin filtering, with a voltage applied to the

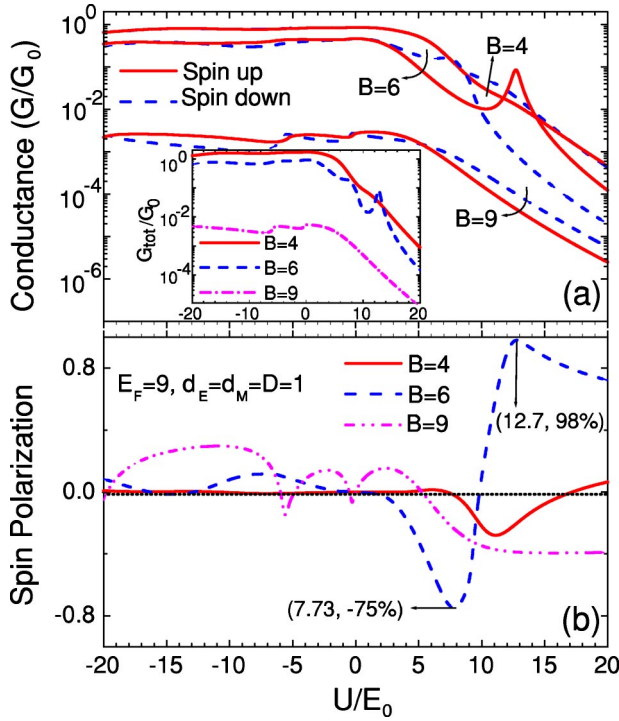


FIG. 4. Spin-dependent conductance and spin polarization versus the electric potential strength U under the Schottky metal stripe, for the same device as in Figs. 2 and 3. The total conductance is plotted in the inset. Three magnetic field strengths, $B=4, 6$ and 9 , are considered. Other device parameters used are $d_M=d_E=D=1$ and $E_F=9$.

Schottky NM stripe, in the device considered here. In Fig. 4 the conductance and spin polarization are plotted as a function of the EB height at a given Fermi energy ($E_F=9$) for three fixed MB strengths ($B=4, 6, 9$). From the lower panel one can observe that only for suitable MB strengths the spin polarization may exhibit a drastic variation with increasing the EB height. For example, at the MB strength of $B=6$, when the EB potential is changed from $U=7.7$ to $U=12.7$, the polarization varies from -75% to 98% . Within this EB potential region the system can produce a strong spin-polarized current with either spin orientation. A FM stripe with a stronger magnetization ($B > 2\sqrt{2E_F}$) does not necessarily lead to a more pronounced spin polarization in the device. This is reasonable because in this case the k_y -dependent magnetic vector potential barrier is high compared with the considered EB potential and thus the symmetry in the device, with respect to the operation of $\hat{T}\hat{R}_x\hat{R}_y$, is difficult to break. On the other hand, when the magnetization strength of the FM stripe is weak, the effect of the magnetic field on the electron motion and the Zeeman energy are small, and therefore no strong spin polarization can be expected (see, e.g., the $B=4$ case in Fig. 4). Another observation from Fig. 4(b) is that for all negative values of U the polarization is small in the device. This is true as long as the Fermi energy is sufficiently large (cf. Fig. 5).

The above analysis gives a qualitative picture about spin polarization in the device with a double metal stripe structure. In a realistic case, instead of the simple double-spike-

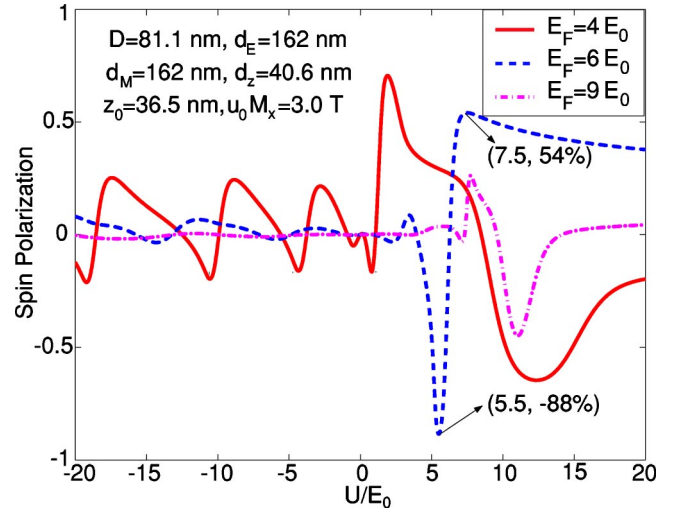


FIG. 5. Spin polarization versus the electric potential strength U for the double metal stripe device with a realistic magnetic field configuration, as shown by the dashed line in Fig. 1(b), induced by a FM stripe placed at a distance of $z_0=16.2$ nm on top of the InAs 2DEG. The FM stripe has a rectangular cross section of height $d_z=40.6$ nm and width $d_M=162$ nm, and magnetization $\mu_0 M_x=3.0$ T. The calculations are carried out for the Fermi energy $E_F=4E_0$ (solid line), $E_F=6E_0$ (dashed line) and $E_F=9E_0$ (dash-dotted line). Other device parameters assumed are $d_E=162$ nm and $D=81.1$ nm.

like form, the modulated magnetic field in the 2DEG has a smooth profile, as shown in Fig. 1(b) (dashed line). For a FM stripe with a rectangular cross section and magnetization along the x -direction, the generated magnetic field profile can be obtained analytically using a formula in Ref. 18. Figure 5 shows the calculation for spin polarization, P_G , of the device with such a FM stripe, whose parameters are given in the figure caption. Note that ferromagnetic elements with a sub-micron scale have been successfully produced on top of a 2DEG,^{19,20} and therefore our considered structure is in the realizable scope of current technology. The calculation shows that the polarization behavior of the device is similar to that seen in Fig. 4(b). The polarization remains large and exhibits rich variations in its amplitude and polarity with increasing the EB height. This is encouraging, because it is indicated that it is the magnetization strength, as well as the width of the FM stripe, rather than the shape of the magnetization profile that has a drastic effect on the polarization characteristics of the spin device proposed here.

All results presented so far are obtained for the zero-temperature case. For an application, it is interesting to know the temperature dependence of the results. The spin-dependent conductance at a finite temperature T_K relates with its zero-temperature values through

$$G_{\sigma_z}(E_F, T_K) = \int_0^{\infty} dE G_{\sigma_z}(E, T_K=0) \left(-\frac{df_{FD}}{dE} \right), \quad (5)$$

where $f_{FD}(E) = \{1 + \exp[(E - E_F)/k_B T_K]\}^{-1}$ is the Fermi-Dirac distribution function. Figure 6 illustrates the influence of the temperature on the spin polarization for the device as in Fig.

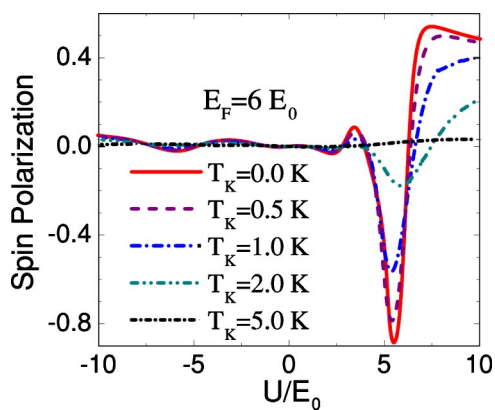


FIG. 6. Spin polarization calculated as a function of the electric potential strength U for the same device as in Fig. 5 at the Fermi energy $E_F=6E_0$ and various temperatures $T_K=0.0, 0.5, 1.0, 2.0$ and 5.0 K.

5, with the Fermi energy at $E_F=6E_0$. It is shown that the polarization is still remarkable as long as the thermal energy $k_B T_K$ is much less than the maximal magnetic splitting, $E_s = g^*(m^*/2m_0)B_z \max$. For the device with the parameters as in Fig. 5, the spin polarization is seen to be greatly reduced or smoothed out by the thermal smearing at $T_K > E_s/4k_B \approx 1.4$ K.

Finally we would like to point out that a FM stripe deposited on top of a 2DEG can generate not only a modulated magnetic field $B_z(x)$, but also an electric potential $U_B(x)$ in the 2DEG.²¹ This electric modulation comes from the Schottky effect and the strain between the FM and semiconductor materials, and usually is symmetric with respect to the center of the stripe. According to the previous analysis, the system with only a single FM stripe should possess no spin

filtering even in the presence of such a symmetric electric potential. However, the presence of the potential $U_B(x)$ can affect the conductance and polarization values of the double metal stripe structure, because of its influence on the energy positions of the spin-dependent resonant transmission peaks. From our numerical simulation, we find that in general a barrier-like $U_B(x)$ lowers the total conductance and improves the polarization amplitude, while a well-like $U_B(x)$ increases the total conductance and diminishes the polarization amplitude. Since $U_B(x)$ can be changed by a voltage gate applied on the FM stripe, these results suggest an additional way of controlling the performance (conductance and polarization) of the device proposed here.

In conclusion, we have shown that a single antisymmetric magnetic barrier does not provide spin-polarized transport in a 2DEG due to the fact that the system possesses a hidden symmetry. The symmetry can be broken by adding an electric barrier parallel to the magnetic barrier. Based on this result, a 2DEG spin device has been proposed, which can be realized by placing on top of the 2DEG a FM stripe and a Schottky NM stripe in a parallel configuration. The spin polarization of the proposed device has been studied by numerical calculations, and discussed in terms of spin-dependent tunneling. It is shown that the device can be used as a highly efficient spin filter with the spin polarity tunable by applying a voltage to the Schottky NM stripe.

This work was supported by the Swedish Research Council (VR) and by the Swedish Foundation for Strategic Research (SSF) through the Nanometer Structure Consortium at Lund University. One of us (Y.G.) acknowledges the support from the Key Basic Research of Tsinghua University (Grant No. J22002005) and the National Key Project of Basic Research Development Plan (Grant No. G2000067107).

*Electronic address: feng.zhai@ftf.lth.se

†Electronic address: Hongqi.Xu@ftf.lth.se

¹S. A. Wolf, D. D. Awschalom, R. A. Buhrman, J. M. Daughton, S. von Molnár, M. L. Roukes, A. Y. Chtchelkanova, and D. M. Treger, *Science* **294**, 1488 (2001).

²A. T. Filip, B. H. Hoving, F. J. Jedema, B. J. van Wees, B. Dutta, and S. Borghs, *Phys. Rev. B* **62**, 9996 (2000).

³G. Schmidt, D. Ferrand, L. W. Molenkamp, A. T. Filip, and B. J. van Wees, *Phys. Rev. B* **62**, R4790 (2000).

⁴R. Fiederling, M. Keim, G. Reuscher, W. Ossau, G. Schmidt, A. Waag, and L. W. Molenkamp, *Nature (London)* **402**, 787 (1999); Y. Ohno, D. K. Young, B. Beschoten, F. Matsukura, H. Ohno, and D. D. Awschalom, *ibid.* **402**, 790 (1999).

⁵B. T. Jonker, Y. D. Park, B. R. Bennett, H. D. Cheong, G. Kioseoglou, and A. Petrou, *Phys. Rev. B* **62**, 8180 (2000).

⁶E. I. Rashba, *Phys. Rev. B* **62**, R16 267 (2000).

⁷H. J. Zhu, M. Ramsteiner, H. Kostial, M. Wassermeier, H.-P. Schönherr, and K. H. Ploog, *Phys. Rev. Lett.* **87**, 016601 (2001).

⁸A. Matulis, F. M. Peeters, and P. Vasilopoulos, *Phys. Rev. Lett.* **72**, 1518 (1994).

⁹See, e.g., H.-S. Sim, G. Ihm, N. Kim, and K. J. Chang, *Phys. Rev. Lett.* **87**, 146601 (2001) and the references therein.

¹⁰A. Majumdar, *Phys. Rev. B* **54**, 11 911 (1996).

¹¹G. Papp and F. M. Peeters, *Appl. Phys. Lett.* **78**, 2184 (2001); G. Papp and F. M. Peeters, *ibid.* **79**, 3198 (2001).

¹²V. N. Dobrovolsky, D. I. Sheka, and B. V. Chernyachuk, *Surf. Sci.* **397**, 333 (1998).

¹³Y. Guo, B. L. Gu, Z. Zeng, J. Z. Yu, and Y. Kawazoe, *Phys. Rev. B* **62**, 2635 (2000).

¹⁴H. Z. Xu and Y. Okada, *Appl. Phys. Lett.* **79**, 3119 (2001).

¹⁵B. Wang, Y. Guo, X. Y. Chen, and B. L. Gu, *J. Appl. Phys.* **92**, 4138 (2002).

¹⁶H. Z. Xu and Z. Shi, *Appl. Phys. Lett.* **81**, 691 (2002); G. Papp and F. M. Peeters, *ibid.* **82**, 3570 (2003); Y. Guo, J. H. Qin, X. Y. Chen, and B. L. Gu, *Chin. Phys. Lett.* **20**, 1124 (2003).

¹⁷A. Slobodskyy, C. Gould, T. Slobodskyy, C. R. Becker, G. Schmidt, and L. W. Molenkamp, *Phys. Rev. Lett.* **90**, 246601 (2003).

¹⁸I. S. Ibrahim and F. M. Peeters, *Phys. Rev. B* **52**, 17 321 (1995).

¹⁹V. Kubrak, F. Rahman, B. L. Gallagher, P. C. Main, H. Henini, C. H. Marrows, and M. A. Howson, *Appl. Phys. Lett.* **74**, 2507

- (1999).
- ²⁰T. Vančura, T. Ihn, S. Broderick, K. Ensslin, W. Wegscheider, and M. Bichler, Phys. Rev. B **62**, 5074 (2000).
- ²¹See, for example, P. D. Ye, D. Weiss, R. R. Gerhardt, M. Seeger, K. von Klitzing, K. Eberl, and H. Nickel, Phys. Rev. Lett. **74**, 3013 (1995).
- ²²H. Q. Xu, Phys. Rev. B **50**, 8469 (1994); see also M. Cahay, M. McLennan, and S. Datta, *ibid.* **37**, 10 125 (1988).